EE568 Project 2: Motor Winding Design & Analysis

Baris Kuseyri

March 31, 2020

Contents

1 Integral-Slot Winding Design: 120 slot / 20 pole

Integral-slot refers to machine topologies in which the number of slots per pole per phase is an integral number. Here, the word integral indicates that the number (number of slots per pole per phase) is a whole number, an undivided quantity. The number of slots per pole per phase for integral slot winding is

$$q = \frac{Q}{2pm} \tag{1}$$

$$q \in N \tag{2}$$

where Q is the number of slots, p is the number of *pole-pairs*, and m is the number of phases.

The integral-slot electric machine analysed through this project is a 120-slot 20-pole machine. An electric machine with such slot/pole ($N_s/2p$) configuration can be constructed in several methods. The machine winding can be single layer (alternate teeth wound), where there is only one side of coil in each stator slot, or double layer(all teeth wound), where there are one side of two different coils in one stator slot. If it is double layer, the *coil-span* can vary. This project adopts a double layer winding design, where each coil spans 6 slots. The *coil-span* is chosen so that the machine is full-pitched, i.e. the coil pitch equals to the pole pitch [1].

1.1 Winding Diagram

The winding diagram shows how the windings are implemented to the slots of the machine. The winding diagram for the machine under inspection can be seen in Figure 1, below.

In Figure 1, above, each pole is indicated with one rectangle, coloured either red or blue, labelled as either N or S. A single *pole-pair* is composed of two adjacent rectangles, one N and one S. In Figure 1, one *pole-pair* is

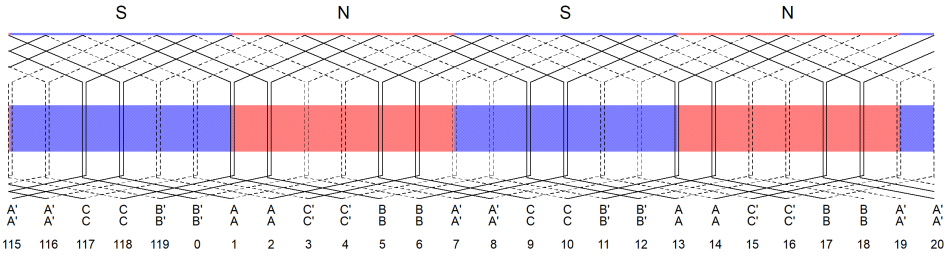

Figure 1: Winding Diagram: 1 pole pair

corresponding to the slots 1 to 13. As can be seen in the figure, every slot has one side of two different coils, indicating that this is a double layer winding. Number of slots per pole per phase is,

$$q = \frac{Q}{2mp} = 2 \tag{3}$$

meaning there are 2 slots (or 4 half-slots) reserved for coils from excited with each phase. In this machine, *coil-span* is set to be 6 slots. Therefore, the 4 half-slots correspond to 2 slots. In Figure 1, for the pole corresponding to slots 1 to 7, the 2 slots reserved for phase A are slot 1 and 2, the first two slots. Winding diagram for 120-slot/20-pole configuration, with a *coil-span* of 6 slots, constructed by the software *Dolomites* can be seen in Figure 2, below. The complete winding diagram is given in Figure 2a and in Figure 2b, the winding diagram corresponding approximately to one *pole-pair* is given. Though the winding diagram presented by the software *Dolomites* does not display how the coils are wounded, the winding diagram in Figure 1 is in compliance with the diagram in Figure 2, in terms of coil sequence.

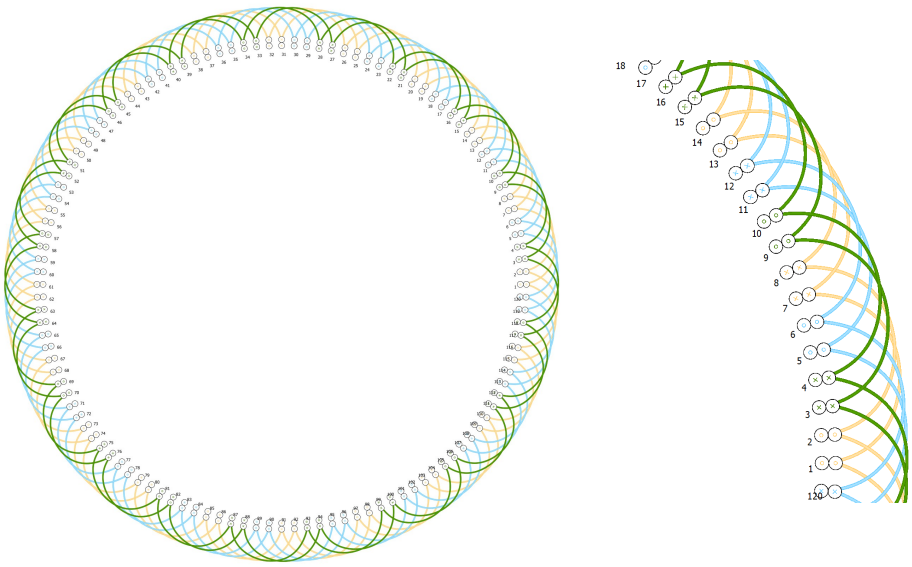

(a) Complete (b) 1 pole-pair

Figure 2: Winding Diagram

1.2 Distribution, Pitch and Winding Factors

The distribution factor is the ration of the effective induced EMF to arithmetic induced EMF. It can be calculated by

$$K_{dn} = \frac{sin\left(n\frac{q\sigma}{2}\right)}{qsin\left(n\frac{\sigma}{2}\right)} \tag{4}$$

where, σ is the electrical angle between two adjacent coils of the same phase, q is the number of coils per phase, and n is the harmonic index. Notice that the distribution factor, based on 4, only depends on the electrical angle between two adjacent coils of the same phase and the number of coils per phase. For an integral-slot winding scheme, the choice of phase coils is rather straightforward. However, this choice becomes complicated for a fractional-slot winding scheme, and is detailed in section 2.1.2.

The pitch factor is the ratio of the effective flux linkage to flux linkage of full-pitched coil. It can be calculated by

$$K_{pn} = \frac{\Psi_s}{\Psi_F} = sin\left(n\frac{\alpha}{2}\right) \tag{5}$$

where, Ψ_e is the effective flux linkage, Ψ_F is the flux linkage of full-pitched coil, α is the electrical angle of coil pitch, and n is the harmonic index. If the coil is full-pitched, then the electrical angle of coil pitch equals to electrical angle of pole pitch (electrical angle pole pitch always equals to 180°). In this case, coil links the fundamental and all harmonic flux components. As a result, the coil pitch equals to 1. In case of short pitch or long pitch, the electrical angle of coil pitch differs from electrical angle pole pitch by an electrical angle A. This angle, and the corresponding pitch factor is same for both short and long pitch coil.

The winding factor is the ratio of the effective winding turns to actual winding turns. It can be calculated by

$$K_{wn} = K_{dn}K_{pn} \tag{6}$$

Distribution, pitch, and the winding factors for 120-slot/20-pole machine is given in Figure 3, for n=1,3,...,21. Additionally, the fundamental and the 3^{rd} and 5^{th} harmonics for each factor are given in Table 1. These factors values are identical to those presented by the software *Dolomites* and the website *Emetor*.

n	1	2	2
Distribution Factor	0.9659	0.7071	0.2588
Pitch Factor	1	1	1
Winding Factor	0.9659	0.7071	0.2588

Table 1: Distribution, Pitch and Winding Factor for $N_s/2p = 120/20$

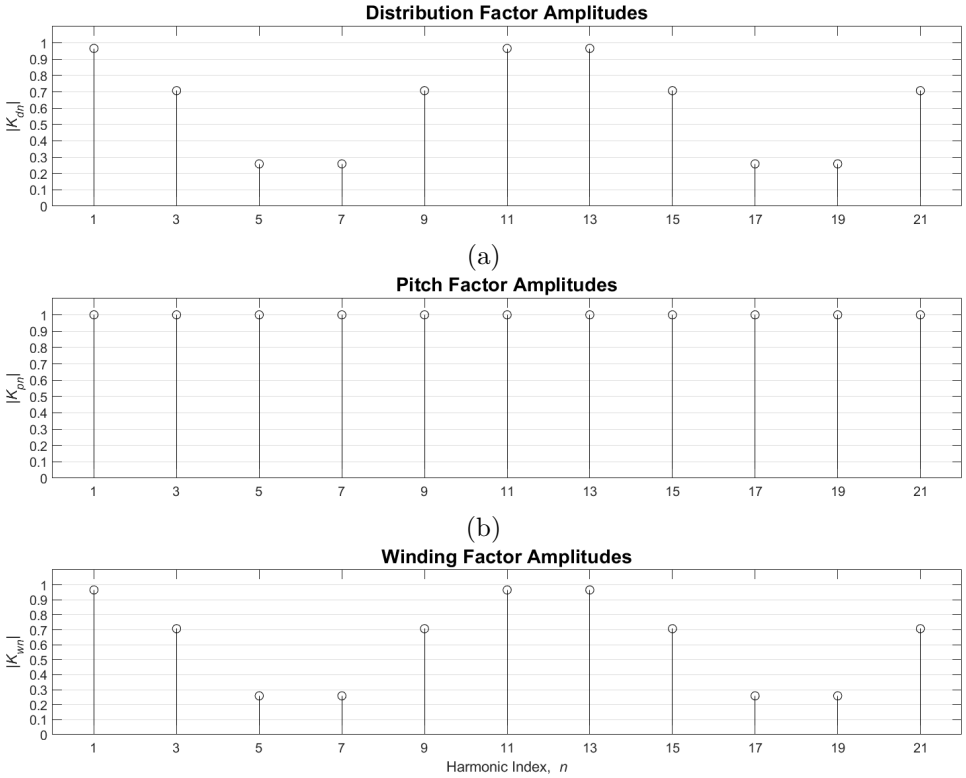

(a)

(b)

(c)

Figure 3: Distribution, Pitch and Winding Factor for $N_s/2p = 120/20$

It is expected to have a unit pitch factor, while the *coil-span* of the machine is selected to be 6 slots, which equals to the pole span, which is $Q/2p = 6$ slots.

The fundamental component of distribution factor is high, an important aspect for an integral slot winding, as it is directly proportinal to sunisoidality of the MMF, however, the 3^{rd} and 5^{th} harmonic components alters the MMF waveform away from a perfect sunisoidal form; thus, not desired. Here, for the $N_s/2p = 120/20$ configuration, the fundamental component of the winding factor is $K_{w1} = 0.9659$, high and well above acceptable levels. However, 3^{rd} and 5^{th} harmonic components of the winding factor are $K_{w3} = 0.7071$ and $K_{w5} = 0.2588$, which are high, deforming the waveform away from its sinusiodality. A scaled MMF waveform according to the fundamental, 3^{rd} and 5^{th} harmonic component values given in Table 1 can be seen in Figure 4.

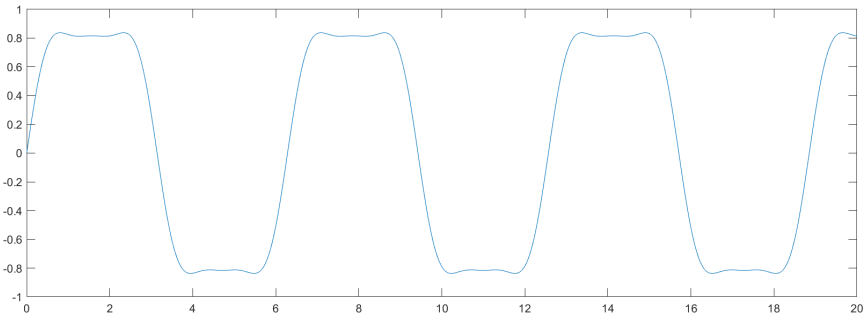

Figure 4: Waveform with $N_s/2p = 120/20$ winding factors (1^{st}, 3^{rd} and 5^{th})

2 Fractional-Slot Winding Design

Fractional-slot refers to machine topologies in which the number of slots per pole per phase is an fractional number.

$$q = \frac{Q}{2pm} \tag{7}$$

$$q \notin N \tag{8}$$

2.1 27-slot/22-pole EM

The first fractional-slot electric machine analysed in this project is a 27-slot 22-pole machine. An electric machine with such slot/pole ($N_s/2p$) configuration can only be constructed as double-layer (all teeth wound). In a double-layer design, the *coil-span* can vary. This project adopts a design where each coil spans 1 slots. This choice depends on the theory that the coil pitch needs to be closer to the pole pitch to obtain a higher pitch factor. Here, *pole-pitch* is $2\pi/2p$ and *slot-pitch* is $2\pi/sQ$, where s is the *coil-span*. Therefore, to obtain the highest pitch factor, *coil-span* is chosen to be 1.

2.1.1 Phase Angle of Induced Voltage in each Slot

The phase shift between each coil can be calculated as

$$phaseshift = \frac{2\pi}{Q/2p} \tag{9}$$

Phase angles of the induced voltages in each slot are presented in Table 2, below.

Slot Number	1	2	3	4	5	6
Phase Angle (°)	0	146.67	293.33	80	226.67	13.33
	7	8	9	10	11	12
	160	306.67	93.33	240	26.67	173.33
	13	14	15	16	17	18
	320	106.67	253.33	40	186.67	333.33
	19	20	21	22	23	24
	120	266.67	53.33	200	346.67	133.33
	25	26	27			
	280	66.67	213.33			

Table 2: Phase angle of the induced voltage for $N_s/2p = 27/22$

2.1.2 Phasor Diagram

One method to represent the main EMF harmonic which are being induced at the coil side is referref as star of slots. The star of slots method uses phasors to represent the EMFs and this representation comprises each of the slots [3].

The star of slots representation method is used to represent the machine with $N_s/2p = 27/22$. The representation with mechanical angles can be seen in Figure 5a, with electrical angles can be seen in Figure 5b. The star of slots representation with electrical angles implements the phasors according to the phase angle values presented in Table 2

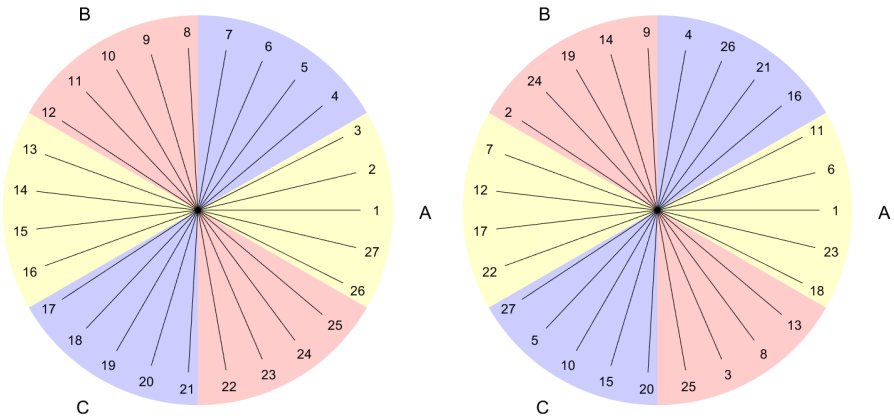

(a) mechanical (b) electrical

Figure 5: Star of Slots for $N_s/2p = 27/22$

Once the star of slots representation with electrical angles is completed, the coils for each phase are selected. This selection is done according to which phasors lie on which $2\pi/6$ area. As can be seen in Figure 6, The slots

corresponding to the phasors which lie on the yellow, or phase A area, are chosen to be wound with phase A coils.

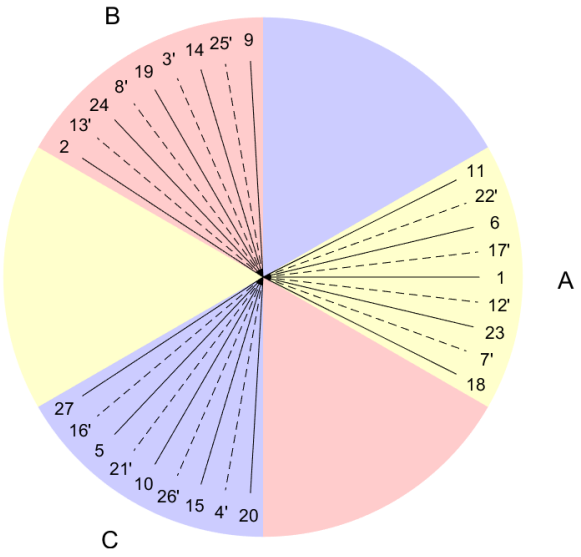

Figure 6: Star of Slots for $N_s/2p = 27/22$ (according to the coil direction)

Finally, the phasor can be represented with a phasor diagram, where phasors from each phase are displayed in an additive manner. The phasor diagram for phase A for the $N_s/2p = 27/22$ topology can be seen in Figure 7.

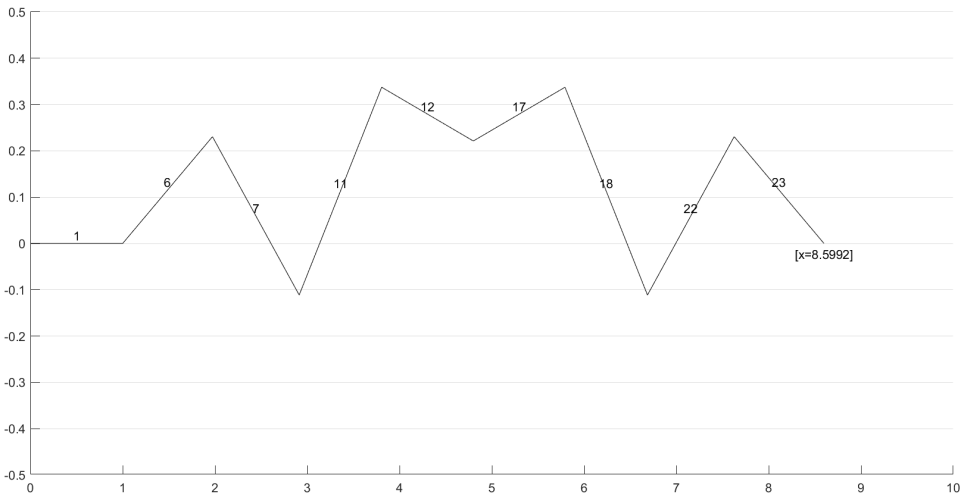

Figure 7: Phasor Diagram for $N_s/2p = 27/22$ (phase A)

It is important to note here that the distribution factor can be deduced

from the phasor diagram. Notice that there are 9 phasors in phase A, which corresponds to arithmetic induced EMF, scaled by peak induced EMF per coil. These phasors add up to the point [x,y]=[8.5992], which corresponds to effective induced EMF. Thus, the distribution factor is

$$K_{dn} = \frac{effectiveinducedEMF}{arithmeticinducedEMF} = \frac{8.5992}{9} = 0.9555 \tag{10}$$

2.1.3 Distribution, Pitch and Winding Factors

Distribution, pitch, and the winding factors for 27-slot/22-pole machine is given in Figure 8, for n=1,3,...,21. Additionally, the fundamental and the 3^{rd} and 5^{th} harmonics for each factor are given in Table 3. These factors values are identical to those presented by the software *Dolomites* and the website *Emetor*.

n	1	2	2
Distribution Factor	0.9555	0.6399	0.1937
Pitch Factor	0.9580	0.6428	0.1161
Winding Factor	0.9153	0.4113	0.0225

Table 3: Distribution, Pitch and Winding Factor for $N_s/2p = 27/22$

As can be seen in Figure 3, the fundamental distribution factor calculated analytically with the Equation 4 gives the same results with that calculated by the phasor diagram in 2.1.2.

2.2 24-slot/22-pole EM

The second fractional-slot electric machine analysed in this project is a 24-slot 22-pole machine. An electric machine with such slot/pole ($N_s/2p$) configuration can only be constructed either as single-layer (alternate teeth wound) or double-layer (all teeth wound). In a double-layer design, the *coil-span* can vary. This project adopts a double-layer design, where each coil spans 1 slots. The choice of *coil-span* is done with the same grounds explained in Subsection 2.1.

2.2.1 Phase Angle of Induced Voltage in each Slot

Phase angles of the induced voltages in each slot are presented in Table 4, below.

2.2.2 Phasor Diagram

The star of slots method and the phasor diagram is completed for the machine with $N_s/2p = 24/22$. The results can be seen in Figure 9, 10 and

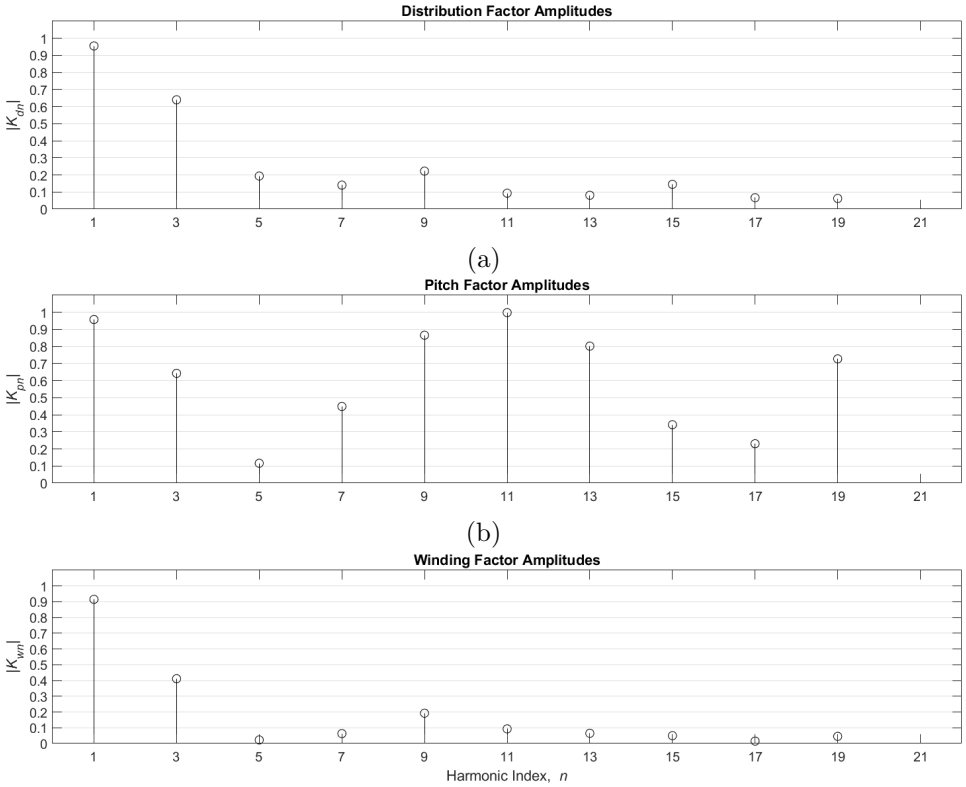

(a)

(b)

(c)

Figure 8: Distribution, Pitch and Winding Factor for $N_s/2p = 27/22$

Slot Number	1	2	3	4	5	6
Phase Angle (°)	0	165	330	135	300	105
	7	8	9	10	11	12
	270	75	240	45	210	15
	13	14	15	16	17	18
	180	345	150	315	120	285
	19	20	21	22	23	24
	90	255	60	225	30	195

Table 4: Phase angle of the induced voltage

11 displayed below.

Again, the distribution factor can be deduced from the phasor diagram here. Notice that there are 8 phasors in phase A, which corresponds to arithmetic induced EMF, scaled by peak induced EMF per coil. These phasors add up to the point [x,y]=[7.6613], which corresponds to effective induced EMF. Thus, the distribution factor is

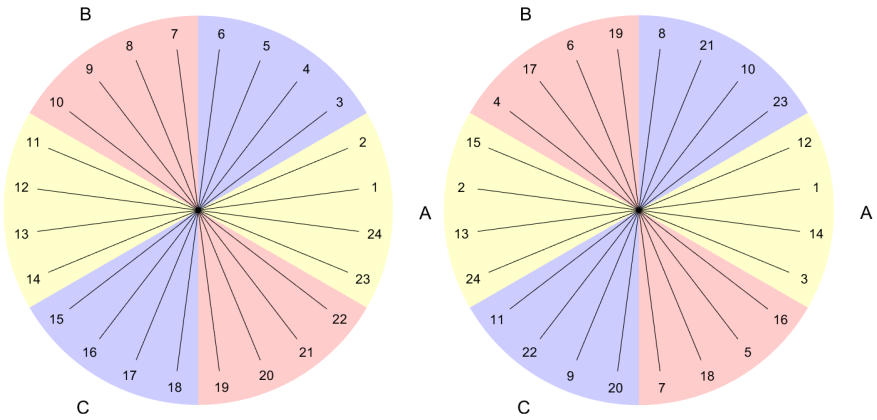

(a) mechanical (b) electrical

Figure 9: Star of Slots for $N_s/2p = 24/22$

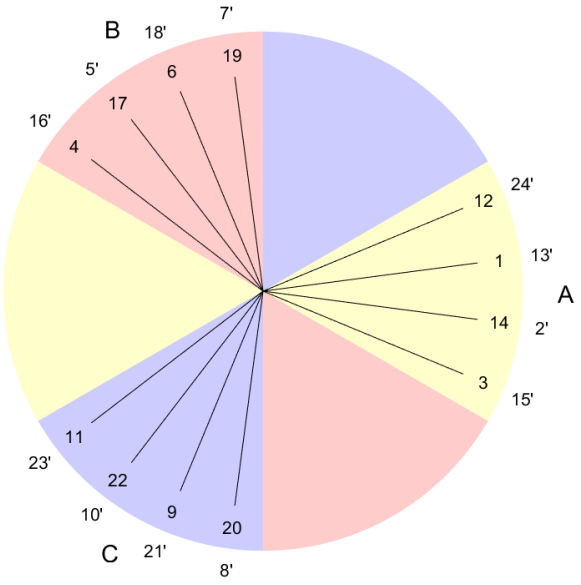

Figure 10: Star of Slots for $N_s/2p = 24/22$ (according to the winding direction)

$$K_{dn} = \frac{effectiveinducedEMF}{arithmeticinducedEMF} = \frac{7.6613}{8} = 0.9577 \tag{11}$$

2.2.3 Distribution, Pitch and Winding Factors

Distribution, pitch, and the winding factors for 24-slot/22-pole machine is given in Figure 12, for n=1,3,...,21. Additionally, the fundamental and

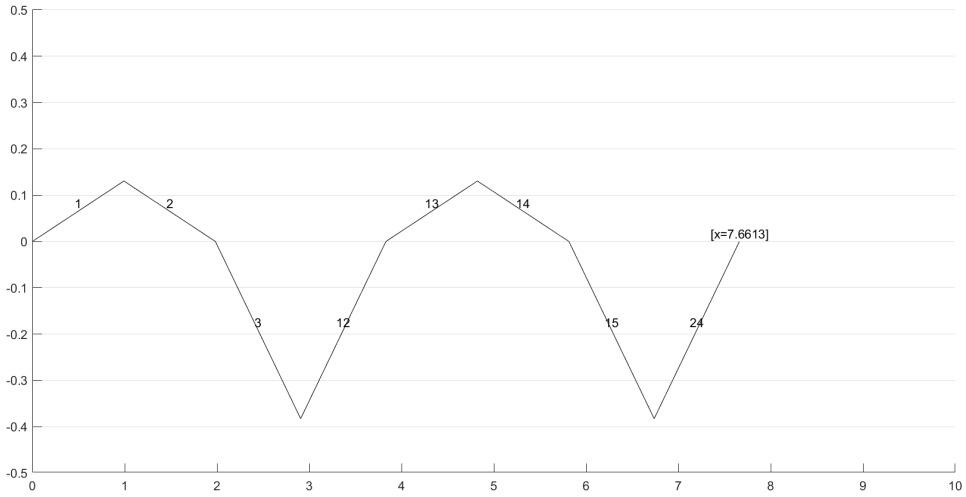

Figure 11: Phasor Diagram for $N_s/2p = 27/22$ (phase A)

the 3rd and 5th harmonics for each factor are given in Table 5. These factors values are identical to those presented by the software *Dolomites* and the website *Emetor*.

n	1	2	2
Distribution Factor	0.9577	0.6533	0.2053
Pitch Factor	0.9914	0.9239	0.7934
Winding Factor	0.9495	0.6036	0.1629

Table 5: Distribution, Pitch and Winding Factor for $N_s/2p = 24/22$

Again here, as can be seen in Figure 5, the fundamental distribution factor calculated analytically with the Equation 4 gives the same results with that calculated by the phasor diagram in 2.2.2.

2.3 Evaluation

Fundamental component winding factor is very similar in these two designs, though higher for $N_s/2p = 24/22$ than $N_s/2p = 27/22$, i.e $K_{w1} = 0.9495$ for $N_s/2p = 24/22$ and $K_{w1} = 0.9153$ for $N_s/2p = 27/22$, as can be seen in Table 3, 5. Fundamental component of pitch factor for $N_s/2p = 24/22$ is $K_{p1} = 0.9914$, while for $N_s/2p = 27/22$ it is $K_{p1} = 0.9580$. The fundamental component of the distribution factors are very similar, i.e. $K_{d1} = 0.9577$ for $N_s/2p = 24/22$ and $K_{d1} = 0.9555$ for $N_s/2p = 27/22$. Therefore, pitch factors are the main contributers to this result.

The 3rd and the 5th harmonic component of winding factor diminish faster for the design with $N_s/2p = 27/22$ than $N_s/2p = 24/22$, as can be seen

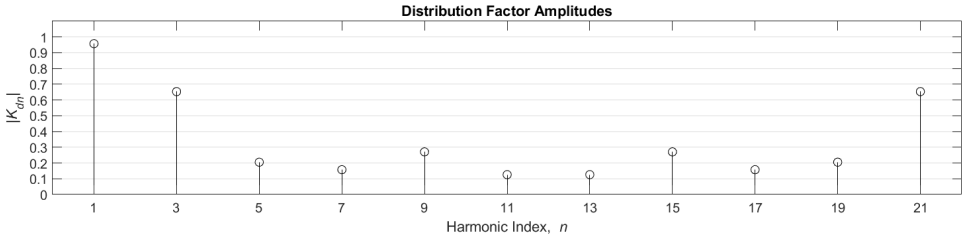

(a)

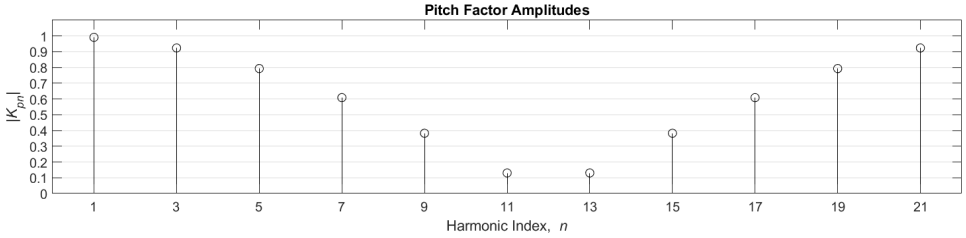

(b)

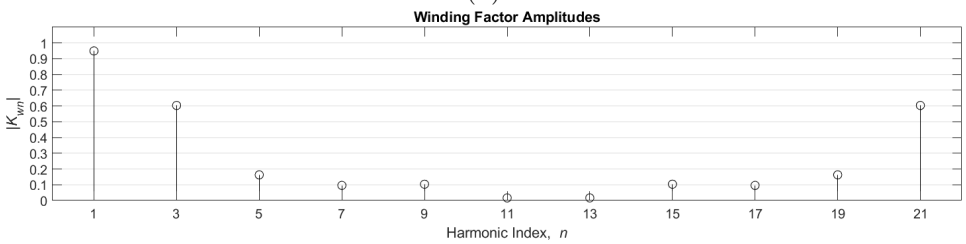

(c)

Figure 12: Distribution, Pitch and Winding Factor for $N_s/2p = 24/22$

in Figure 8c, 12c and Table 3, 5. In case of $N_s/2p = 24/22$, the winding factor decreases from $K_{w1} = 0.9495$ at fundamental component, to $K_{w3} = 0.6036$ at 3^{rd} harmonic, and then to $K_{w5} = 0.1629$ at 5^{th} harmonic, while in case of $N_s/2p = 27/22$, the winding factor decreases from $K_{w1} = 0.9153$ at fundamental component, to $K_{w3} = 0.4113$ at 3^{rd} harmonic, and then to $K_{w5} = 0.0225$ at 5^{th} harmonic. This is again the result of pitch factor values at 3^{rd} and 5^{th} harmonic component. The distribution factor decreases in similar fashion for both $N_s/2p = 27/22$ and $N_s/2p = 24/22$. However, the pitch factor plummets at 5^{th} harmonic component for $N_s/2p = 27/22$, while it takes almost 11^{th} harmonic for $N_s/2p = 24/22$ pitch factor to decrease to that levels.

The fundamental component distribution factors for both designs are similar. This was expected after constructing the single phase phasor diagram for $N_s/2p = 27/22$ in Figure 7. The phasor diagram for $N_s/2p = 27/22$ contains 9 phasors, one more phasor than that for $N_s/2p = 24/22$, which has 8 phasors. The phasor diagram for $N_s/2p = 27/22$ has one extra phasor that is in the same direction as phase A, which increases the distribution factor.

However, the phasors spread further away from phase A in $N_s/2p = 27/22$, as can be seen in Figure 6, 10. This, in turn, decreases the distribution factor. Overall, the two adjustments happen on the phasors as the design changes from $N_s/2p = 27/22$ to $N_s/2p = 24/22$ have opposite effects on distribution factor, working against each other. Thus the overall effect on distribution factor is small.

3 2-D FEA Modelling: 27-slot/22-pole EM

The machine with $N_s/2p = 27/22$ winding design is modelled in 2 dimensions. *ANSYS RMxprt* is used to model the machine. The parameters presented at *Chapter 10: Examples* of Hanselman's book are adopted as the design parameters [2]. Overall, the machine simulation results present an efficiency of %71.4257 at full-load operation. This efficiency rating is less than the general efficiency ratings achieved with permanent magnet synchronous machines; therefore, the model needs further optimization.

Electrical Steel	M19 M4G	Rated Output Power	20 kW
Stacking Factor	0.95	Rated Voltage	138
Conductors per Slot	52	Rated Speed	1000 rpm
Winding Factor	0.9495	Operating Temperature	50°
Magnet Type	Arnold Magnetics N45	°	

Table 6: Machine Parameters

3.1 2-D drawing and winding diagram

The 2 dimensional model as it is depicted in the simulation environment can be seen in Figure 13, below.

The winding diagram as it is depicted in the simulation environment can be seen in Figure 15, below. It is apparent that each coil spans 1 slot.

3.2 Airgap flux density distribution

The airgap flux density is plotted by the *RMxprt* simulation and can be seen in Figure 16, below. It can be seen that the airgap flux density varies between $-0.82T$ and $0.82T$.

3.3 Induced voltage waveforms (for phase and line-to-line) at rated speed

The induced voltage waveforms (for phase and line-to-line) at rated speed are plotted by the *RMxprt* simulation and can be seen in Figure 17, below.

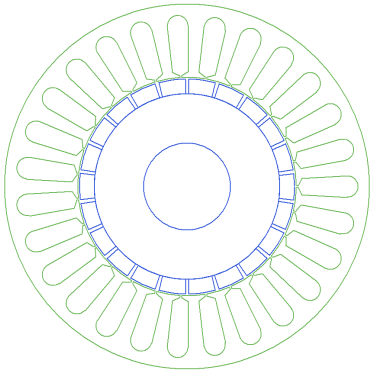

Figure 13: General 2-D Drawing

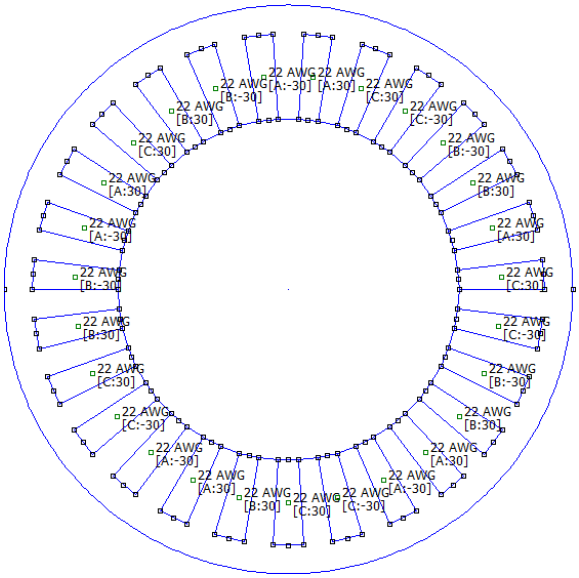

Figure 14: Stator 2-D Drawing (FEMM)

3.4 Cogging torque

The cogging torque is plotted by the *RMxprt* simulation and can be seen in Figure 18, below. As can be seen in Figure 18b, cogging torque varies between $0.013Nm$ and $-0.013Nm$. The rated torque at full-load operation is obtained as $15.6622Nm$ from the software. Therefore, the cogging torque is %0.08 of the rated torque.

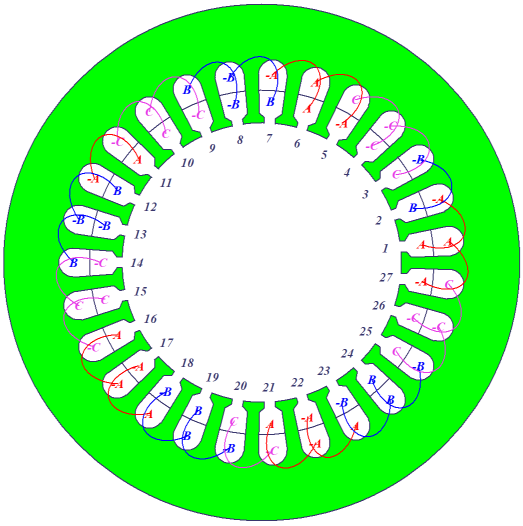

Figure 15: Winding Diagram

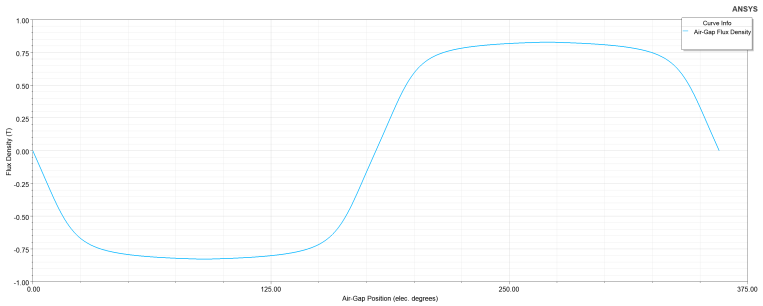

Figure 16: Airgap Flux Density

References

[1] David Howe Dalaman Ishak, Zi-Qiang Zhu. Comparison of pm brushless motors, having either all teeth or alternate teeth wound. *IEEE Transactions on Energy Conversion*, 21(1):95–103, 3 2006.

[2] Duane C. Hanselman. *Brushless Permanent Magnet Motor Design*. Magna Physics Publishing, 3000 M Henkle Drive, Lebanon, Ohio 45036", 2 edition, 2006.

[3] Michele Dai Pre Nicola Bianchi. Use of the star of slots in designing fractional-slot single-layer synchronous motors. *IEE Proceedings - Electric Power Applications*, 153(3):459–466, 5 2006.

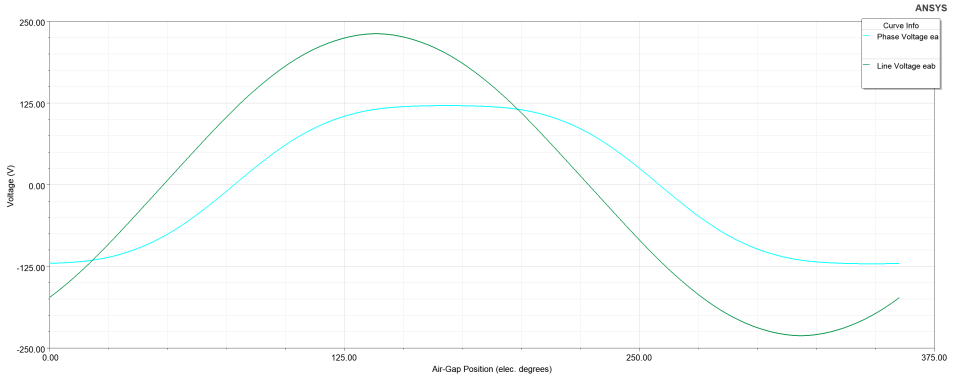

Figure 17: Induced Voltage Waveforms (for phase and line-to-line) at rated speed)

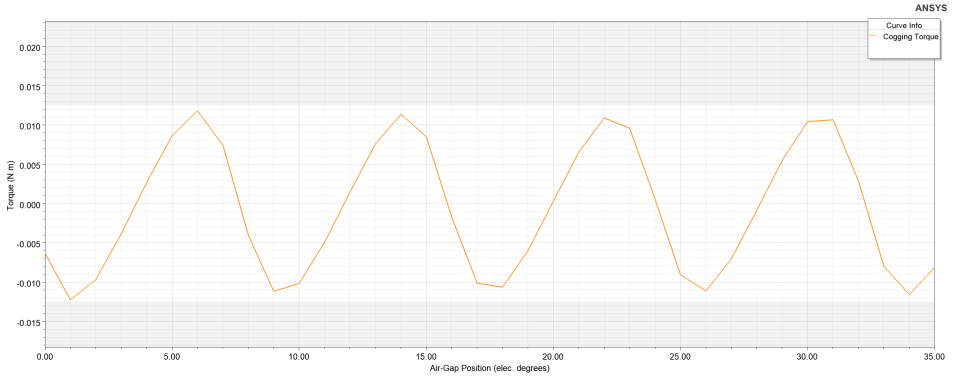

(a)

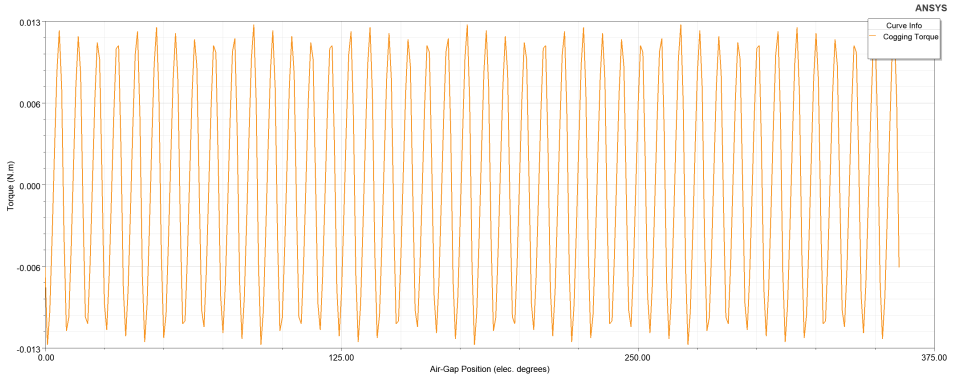

(b)

Figure 18: Cogging Torque in two Teeth